

# Inverse correlation of the up-regulation of FZD10 expression and the activation of $\beta$ -catenin in synchronous colorectal tumors

Satoshi Nagayama,<sup>1,6,7</sup> Eiji Yamada,<sup>1,2,6</sup> Yoshiki Kohno,<sup>2,3</sup> Tomoki Aoyama,<sup>2</sup> Chikako Fukukawa,<sup>4</sup> Hajime Kubo,<sup>1</sup> Go Watanabe,<sup>1</sup> Toyomasa Katagiri,<sup>4</sup> Yusuke Nakamura,<sup>4</sup> Yoshiharu Sakai<sup>1</sup> and Junya Toguchida<sup>2,5</sup>

<sup>1</sup>Department of Surgery, Graduate School of Medicine, Kyoto University, Kyoto 606-8507; <sup>2</sup>Department of Tissue Regeneration, Institute for Frontier Medical Sciences, Kyoto University, Kyoto 606-8507; <sup>3</sup>Department of Orthopaedic Surgery, Graduate School of Medicine, Kyoto University, Kyoto 606-8507; <sup>4</sup>Laboratory of Molecular Medicine, Human Genome Center, The Institute of Medical Science, University of Tokyo, Tokyo 108-8639; <sup>5</sup>Center for iPS Research and Application, iCeMS, Kyoto University, Kyoto 606-8507, Japan

(Received July 8, 2008/Revised November 4, 2008/Accepted November 12, 2008/Online publication January 1, 2009)

We investigated the immunohistochemical expression patterns of Frizzled homolog 10 (FZD10), a cell-surface receptor for molecules in the Wnt pathway, in tissue samples derived from 104 patients with colorectal cancers (CRCs). There was no immunoreactivity for FZD10 in normal colonic mucosa, and only tumor cells in polyps and CRC tissues showed spotted immunostaining patterns in apical sides of the cytoplasm. In metastatic liver lesions, tumor cells showed cytoplasmic immunostaining similar to primary lesions, whereas normal liver parenchyma showed almost no immunostaining. Frequencies of FZD10-immunopositive cells in tumor tissues were significantly higher in CRCs than those in polyps ( $3.3 \pm 10.3\%$  vs  $20.5 \pm 31.7\%$ ,  $P = 0.0016$ ), and almost equivalent with those in metastatic liver lesions ( $33.2 \pm 39.7\%$  vs  $26.4 \pm 33.4\%$ ,  $P = 0.133$ ). Analyses of paired samples (polyps and CRCs, or CRCs and metastatic liver lesions from the same patient) suggested that a subset of CRCs possessed intrinsic genetic mechanisms causing the evolution of FZD10-positive clones during tumor progression, making FZD10 a promising candidate for molecular imaging and a target for therapy. To our surprise, cancer cells immunopositive for FZD10 showed significantly less nuclear accumulation of  $\beta$ -catenin, compared to FZD10-immunonegative cancer cells, and there was a strong inverse correlation between nuclear immunostaining scores for  $\beta$ -catenin expression and expression patterns of FZD10 ( $P = 0.0002$ ), suggesting that FZD10 has a distinct role from other FZDs in canonical Wnt signal transduction. (*Cancer Sci* 2009; 100: 405–412)

The Wnt signal pathway is an essential signal pathway for multicellular organisms with diverse biological consequences. A large number of components are involved in signal transduction, one of which is the Frizzled homolog protein (FZD) that serves as a seven-pass transmembrane receptor for Wnt ligands. So far 10 members of FZD family genes have been identified based on structural and functional homologies. Colorectal cancers (CRCs) are prototype tumors and the Wnt signal pathway is profoundly involved in CRC pathogenesis. There are two major intracellular pathways of Wnt signal transduction: canonical and non-canonical pathways. In the early stages of CRC progression, Wnt signal activation frequently appears due to genetic alterations of molecules in the Wnt canonical pathway including Adenomatous polyposis coli (APC) and  $\beta$ -catenin, resulting in the stabilization and nuclear translocation of  $\beta$ -catenin with the subsequent transcriptional activation of Wnt target genes.<sup>(1–6)</sup> In contrast to extensive studies related to downstream events of Wnt signal transduction, little attention has been paid to the specificity of FZD receptors in CRCs, although there have been a few reports demonstrating the up-regulation of FZD1 and FZD2 in poorly differentiated CRCs,<sup>(7)</sup> and FZD7 expression in colon cancer cell lines with APC or  $\beta$ -catenin mutations.<sup>(8)</sup>

We previously demonstrated that FZD10, the latest cloned member of the FZD family, was specifically up-regulated in synovial sarcomas based upon a genome-wide analysis of gene-expression profiles in soft-tissue sarcomas.<sup>(9)</sup> Since FZD10 is located in plasma membranes and its expression is very low or absent in vital organs, we focused on this molecule as a likely candidate for antibody-based therapy, and demonstrated the therapeutic potential of antibodies directed against FZD10 in synovial sarcomas.<sup>(10,11)</sup> Although FZD10 protein expression patterns in tumor tissues were not demonstrated, and the precise biological behavior of FZD10 with regard to tumorigenesis of CRCs remains obscure, the up-regulation of FZD10 mRNA was observed in two out of 11 cases with primary CRCs.<sup>(12)</sup>

Using a specific monoclonal antibody directed against FZD10, we analyzed expression patterns of FZD10 in colonic polyps, primary CRCs, and metastatic liver lesions to elucidate the role of FZD10 in the progression of CRCs. In addition, we examined the relationship between expression patterns of FZD10 and  $\beta$ -catenin, which is the main signal transducer of the canonical Wnt pathway.

## Materials and Methods

**Tissue samples and cell lines.** Tissue samples were obtained from 104 CRC patients that had undergone surgical curative resection at the Department of Surgery, Kyoto University Hospital during 1999–2001 (Table 1). All samples were approved for analysis by the ethics committee of the Faculty of Medicine of Kyoto University. Formalin-fixed and paraffin-embedded samples were obtained from all patients, and were subdivided into the three following groups: (1) only primary tumor samples were available in 57 cases; (2) paired polyps were available in 30 cases; (3) paired, synchronous metastatic liver lesions were available in the remaining 17 cases. Frozen tissue samples were obtained from 15 patients, which were snap-frozen in liquid nitrogen immediately after resection and stored at  $-80^{\circ}\text{C}$  until further use. Cell lines derived from synovial sarcomas (HS-SY-II, YaFuSS, and SYO-1),<sup>(9)</sup> and colon cancers (SW480, LoVo, and SNU-C4) were grown in monolayers in appropriate media supplemented with 10% fetal bovine serum and 1% antibiotic/antimycotic solutions.

**Monoclonal antibodies (MAbs) directed against FZD10.** A recombinant extracellular domain (rECD) of FZD10 (residues 1–225) was prepared using a pET expression vector with *Escherichia*

<sup>6</sup>These authors contributed equally to this work.  
<sup>7</sup>To whom correspondence should be addressed.  
E-mail: nagayama@kuhp.kyoto-u.ac.jp

**Table 1. Classification of samples used in immunohistochemical analyses**

Subgroup ID	No. of patients	Samples available for the analyses							LM
		N	Polyp	CRC (Duke's classification)				Total	
				A	B	C	D		
1	57	57	None	18	16	23	0	57	None
2	30	30	30	12	10	8	0	30	None
3	17	17	None	0	0	0	17	17	17

CRC, primary colorectal cancer; LM, liver metastasis; N, normal mucosa.

*coli* strain BL21 codonplus (DE3), as previously described.<sup>(10)</sup> Murine anti-FZD10 MAbs were generated by immunizing 4-week-old female Balb/c mice with purified FZD10-rECD recombinant protein (Medical and Biological Laboratories, Nagoya, Japan). Lymph node cells from immunized mice were then harvested and fused with a myeloma cell line. Hybridomas were subcloned by enzyme-linked immunosorbent assay for their ability to secrete immunoglobulins that bound to the ECD of FZD10. Positive clones were further analyzed for specific binding activity by flow cytometry, and MAbs (6C9) were affinity-purified on a protein G-sepharose column for further characterization.

**Flow cytometry.** Suspensions of  $5 \times 10^6$  cells were incubated with 1.5  $\mu\text{g}$  of 6C9 MAbs or non-immunized mouse IgGs for 30 min at 4°C. After washing with phosphate-buffered saline, 2  $\mu\text{g}$  of fluorescent antimouse IgGs (Alexa Fluor 488; Molecular Probes, Eugene, OR, USA) were added, and cell suspensions were incubated for 30 min at 4°C for analysis by FACScan (Becton Dickinson, San Jose, CA, USA).

**Epitope mapping.** A series of 10-residue linear synthetic peptides that overlapped by one amino acid and covered the entire FZD10-ECD were covalently bound to a cellulose membrane (SPOTs; Sigma Genosys, Woodlands, TX, USA). The membrane contained 216 peptide spots and was hybridized with 6C9 MAbs overnight at 4°C. After incubation with antimouse horseradish-peroxidase-conjugated IgGs, spots were visualized with 3-amino-9-ethylcarbazole.

**Semiquantitative reverse transcription-polymerase chain reaction (RT-PCR).** For RT-PCR experiments, total RNA was extracted from cell lines and frozen surgical specimens using a NucleoSpin kit (Macherey-Nagel, Düren, Germany), and a 3- $\mu\text{g}$  aliquot of each total RNA was reverse-transcribed using a First-Strand cDNA Synthesis Kit (Amersham Biosciences, Piscataway, NJ, USA). Synthesized cDNAs were used as templates in PCR amplifications using specific primers for FZD genes (*FZD1* to *FZD10*), and for  $\beta$ -actin and  $\beta 2$ -microglobulin genes as internal controls, as previously described.<sup>(9,10)</sup> PCR reactions were optimized for a number of cycles to ensure product intensities stayed within the linear phase of amplification. In addition, PCR data were quantified using Scion image analyzing software and the ratios of expression levels of tumors to normal matched samples (T/N) were corrected with expression levels of  $\beta$ -actin and expressed in base two logarithm ( $\log_2$ [T/N]).

**Immunohistochemical analyses.** Immunohistochemical staining was carried out using the Envision plus system (DAKO, Kyoto, Japan) according to the manufacturer's instructions but with minor modifications. Briefly, 5- $\mu\text{m}$  thick sections of 24-h formalin-fixed and paraffin-embedded tissues were deparaffinized, rehydrated, and processed for antigen retrieval by 4-min microwave treatment using a Target-Retrieval Solution (DAKO). Tissue sections were then incubated at 4°C overnight with 5  $\mu\text{g}/\text{mL}$  of 6C9 MAb or 2.5  $\mu\text{g}/\text{mL}$  of  $\beta$ -catenin MAb. Subsequently, a mouse ENVISSION Polymer Reagent (DAKO) was added as a secondary antibody, and visualized with a peroxidase substrate DAB (3, 3'-diaminobenzidine tetrahydrochloride). Nuclei were

counterstained with Mayer's hematoxylin. As negative controls, non-immune mouse IgGs were used as primary antibodies with the same protocol, and human placenta tissues were immunostained simultaneously as positive controls.<sup>(10)</sup> Specimens were examined under Olympus BX50 microscopes (Olympus, Tokyo, Japan). The staining status of FZD10 was evaluated by counting the number (%) of immunoreactive tumor cells for more than 500 tumor cells in more than three fields at  $\times 400$  magnification. In order to examine the expression status of  $\beta$ -catenin in FZD10-positive or -negative cancer cells, immunohistochemical analyses of FZD10 and  $\beta$ -catenin were performed on the same cancer cells using serial sections. For the evaluation of nuclear and cytoplasmic  $\beta$ -catenin immunoreactivity, the intensity of the immunostaining was determined as 0 (negative), 1 (weak), 2 (moderate), or 3 (strong). The frequency of immunoreactive cancer cells was stratified based on the percentage of  $\beta$ -catenin-positive cells for more than 500 FZD10-positive or -negative cells in more than three fields at  $\times 400$  magnification into the following categories: 0 (0%), 1 (0–24%), 2 (25–49%), 3 (50–74%), or 4 (75–100%). Additionally, an immunoreactive score was calculated by multiplying the immunostaining intensity and the percentage of positive cells, as previously proposed.<sup>(13,14)</sup> In the case of heterogeneous staining intensities within one sample, each component was scored independently, and results were summed. Immunohistochemical assessments were performed independently by two investigators (E.Y and S.N) who were blinded to each sample.

**Statistical analyses.** Statistical analyses were performed with StatView-J 4.0 software (SAS Institute, Cary, NC, USA) by unpaired or paired Student's *t*-tests,  $\chi^2$ -tests and Mann-Whitney tests between two groups and ANOVA for comparison among the three groups. Kaplan-Meier curves were derived to assess the overall survival, and significant differences in survival times among patient subgroups were analyzed using log-rank tests. A statistically significant difference was identified at  $P < 0.05$ .

## Results

**Semiquantitative RT-PCR analyses of FZD10 expression in normal colonic mucosa and CRC tissues.** Expression patterns of the 10 members of the FZD gene family were examined in 15 advanced CRC tissues along with paired normal colonic mucosa (Fig. 1a). Among the 10 members, FZD2, 3, and 6 were expressed relatively higher in tumor tissues as compared to normal mucosa, whereas there were no specific tendencies in expression patterns of FZD1, 4, 5, and 8. Almost no expression of FZD7 was found in specimens examined in this study. In contrast, expression levels of FZD9 and 10 increased markedly in tumor samples as compared to normal matched tissues. Quantified data also indicated a marked up-regulation of the *FZD9* and *10* genes in tumor tissues (Fig. 1b). In particular, the expression of FZD10 was confined to CRC tissues and almost absent from normal mucosa, although expression frequencies of FZD10 in CRC were relatively low in 4/15 cases; these data are compatible with those cited in a previous report.<sup>(12)</sup>

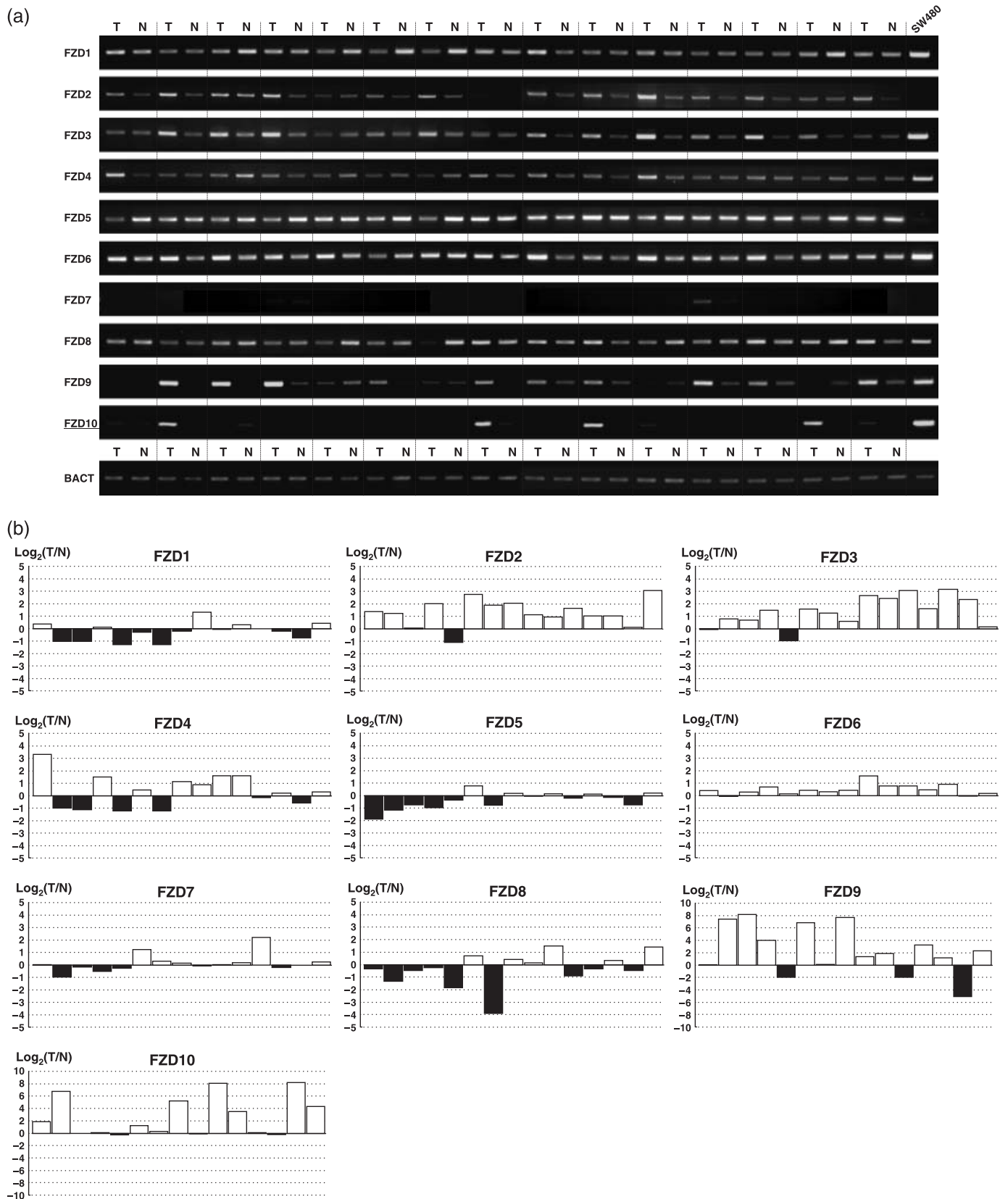


**Fig. 1.** mRNA expression of Frizzled homolog (*FZD*) genes in colorectal cancers (CRCs). (a) Expression patterns of 10 members of *FZD* family genes were analyzed by semiquantitative reverse transcription-polymerase chain reaction (RT-PCR) using 15 pairs of normal mucosa and CRC frozen samples. The expression of  $\beta$ -actin (BACT) served as an internal control, and the SW480 colon cancer cell line was used as a positive control. (b) After quantification of PCR data, the corrected ratios of expression levels of tumors to normal matched samples (T/N) were expressed in base two logarithm ( $\log_2$ [T/N]). Note different scales of expression ratios in *FZD9* and *10*. Open and solid bars show up- and down-regulation of gene expression in tumors as compared to normal matched mucosa, respectively.

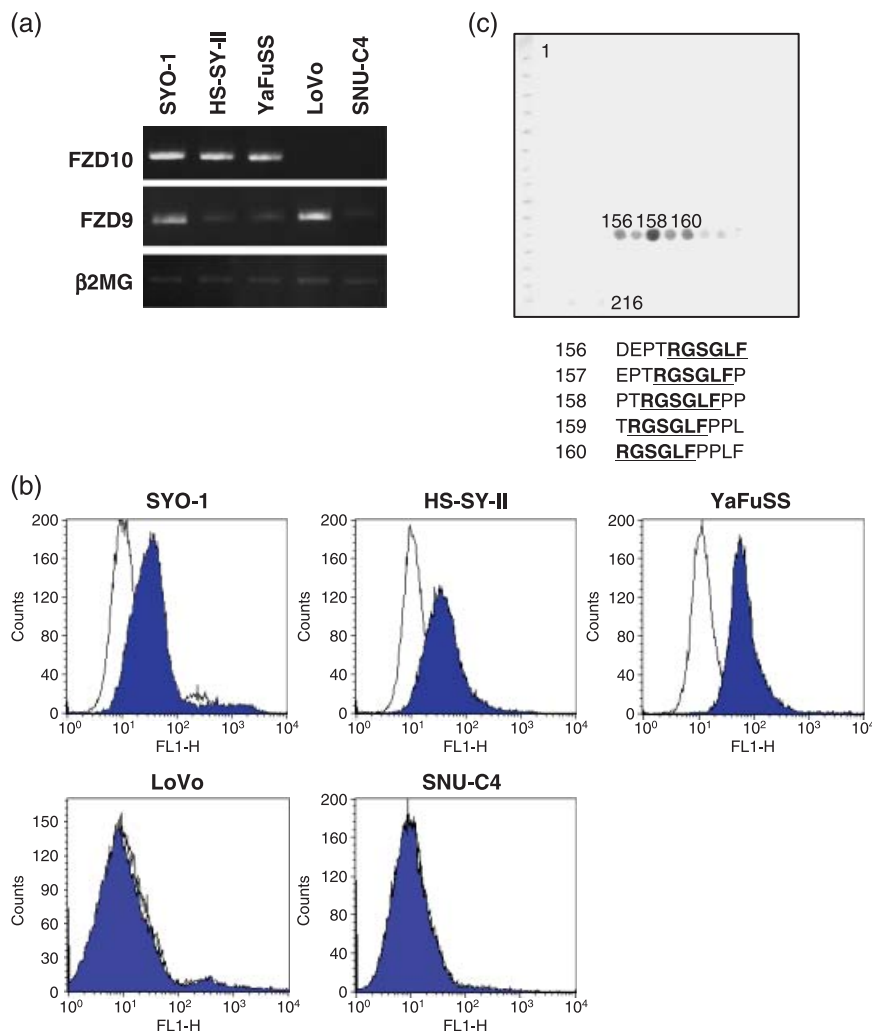


**Fig. 2.** Characterization of monoclonal antibody (MAB) 6C9 for Frizzled homolog 10 (FZD10). (a) Semiquantitative reverse transcription-polymerase chain reaction analyses of mRNA expression of *FZD10* and *FZD9* genes in three synovial sarcoma cell lines (YaFuSS, HS-SY-II, and SYO-1) and two colon cancer cell lines (LoVo, SNUC-1). (b) Flow-cytometric analyses using MAb 6C9. The colored curves show the expression of the cell-surface antigen FZD10 detected by the MAb; the solid lines depict fluorescent signals of cells incubated with non-immunized mouse IgGs as negative controls. The expression of the  $\beta$ 2-microglobulin gene ( *$\beta$ 2MG*) served as an internal control in this RT-PCR analysis. (c) Epitope mapping with overlapping synthetic linear peptides. The 6C9 MAb recognized a single epitope, including a possible core epitope, representing residues 160–165 (RGSGLF) within the N-terminal extracellular domain, indicated by bold letters in the bottom panel.

**Characterization of MAb(6C9) for FZD10.** To assess the binding specificity of 6C9 MABs to FZD10, we performed flow cytometry using five different cell lines whose expression of FZD10 had been predetermined (Fig. 2a). The three cell lines (SYO-1, HS-SY-II, and YaFuSS) with high expression levels of FZD10 were labeled specifically with the 6C9 MAB, whereas there were no labeling curve shifts in FZD10-negative cell lines (LoVo and SNU-C4) (Fig. 2b). These results indicated that the 6C9 MAB specifically recognized the extracellular domain of FZD10 on the cell surface. For further characterization of the MAB, epitope candidates for FZD10 were determined by epitope mapping with overlapping synthetic linear peptides. The MAB 6C9 was found to recognize a single epitope, including a possible core epitope, representing residues 160–165 (RGSGLF) within the N-terminal extracellular domain (Fig. 2c). Taken altogether, we considered the 6C9 MAB to be a specific antibody for FZD10, and used this MAB for further analyses of FZD10.

**FZD10 expression in normal mucosa, polyps, CRCs, and liver metastases.** There was no immunoreactivity observed for FZD10 in normal mucosa (Fig. 3a,c), and only tumor cells in polyps and CRC tissues showed spotted immunostaining patterns in the apical sides of the cytoplasm (Fig. 3b,d). There were no marked differences in the immunostaining intensity among cancer cells, and the distribution of immunostained cancer cells was patchy in some slides. No stromal cells including fibroblasts, macrophages, and endothelial cells were immunostained. In metastatic liver lesions, the normal liver parenchyma showed almost no immunostaining (Fig. 3e), although metastatic cancer cells

showed a similar cytoplasmic immunostaining to CRC tissues (Fig. 3f).

**Association of FZD10 expression with progression of CRCs.** To analyze the significance of FZD10 expression in CRCs, the expression frequency was compared among three groups: (1) 30 cases of colorectal polyps mentioned above (mean age 69.4 years, 15 colon and 15 rectal); (2) 30 CRC cases of Dukes A and B in subgroups 1 and 2 that were followed-up and showed no evidence of recurrence for more than 5 postoperative years (mean age 63.1 years, nine colon and 21 rectal); and (3) 17 CRC cases with synchronous liver metastases mentioned above (mean age 67.3 years, nine colon and eight rectal). There were no significant differences in age and location of tumors among the three groups (Student's *t*-tests and  $\chi^2$ -tests). Significant differences in FZD10 expression patterns were observed among the three groups ( $P = 0.0008$ , ANOVA) (Fig. 4). When comparing two groups, there was a significant increase in Dukes A and B cases ( $13.1 \pm 24.6\%$ ), without lymphogenous or hematogenous metastases, as compared to normal mucosa and colorectal polyps ( $3.3 \pm 10.3\%$ ) ( $P = 0.048$ , Student's *t*-tests). However, expression frequencies were not increased in primary tumors with liver metastases ( $13.1 \pm 24.6\%$  vs  $33.2 \pm 39.7\%$ ) ( $P = 0.071$ , Student's *t*-tests) (Fig. 4).

**FZD10 expression in paired samples.** In order to minimize confounding factors between individuals and to assess the involvement of FZD10 expression in the progression of CRCs, the frequency of FZD10 expression was compared in paired samples derived from a single patient. Although there was only

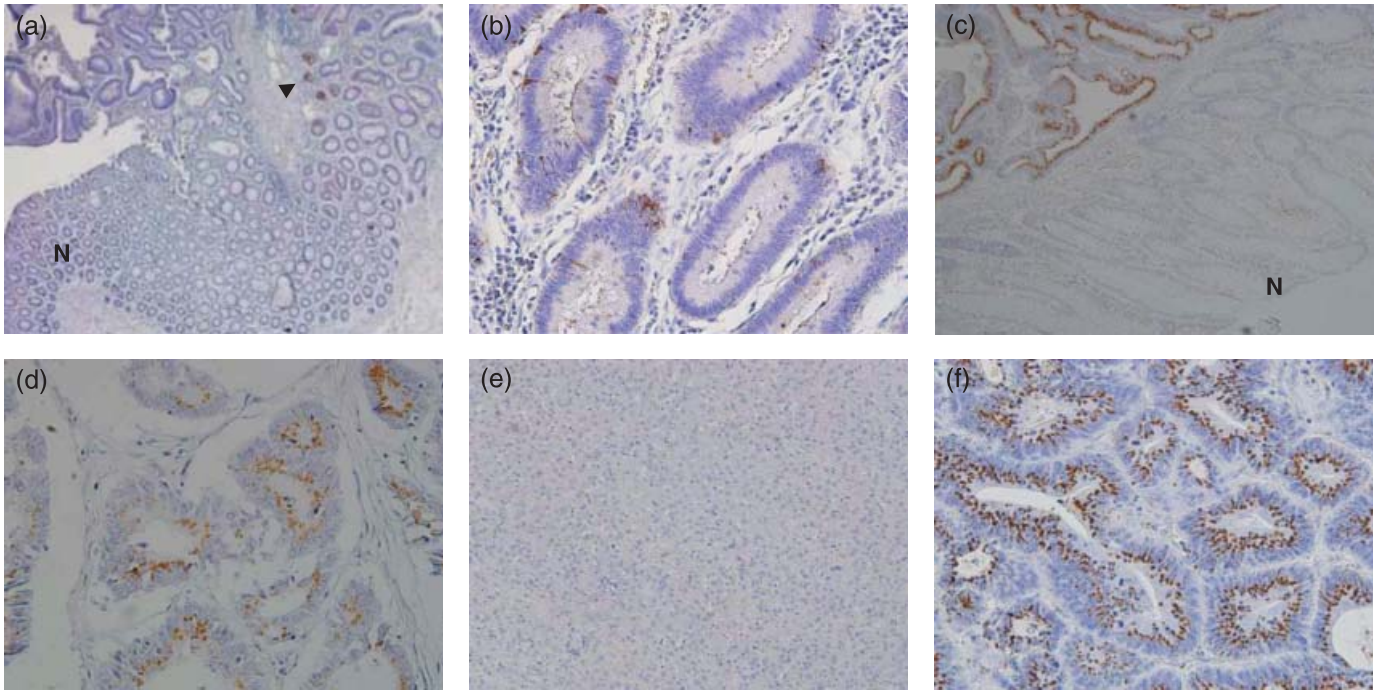


**Fig. 3.** Immunohistochemical analyses for Frizzled homolog 10 (FZD10) expression in colonic polyps, colorectal cancers (CRCs), and metastatic liver lesions. Case A, (a) tubular adenoma and adjacent normal mucosa (N) in a polyp section and (b) tubular adenoma in a higher magnification view; Case B, (c) moderately differentiated adenocarcinoma and adjacent normal mucosa (N) in a CRC section and (d) adenocarcinoma in a higher magnification view; Case C, (e) surrounding normal liver parenchyma and (f) a metastatic adenocarcinoma of colon cancer origin in the same liver section. An arrowhead shows FZD10-immunopositive adenoma cells. Original magnification: (a)  $\times 100$ ; (c, e)  $\times 200$ ; (b, d, f)  $\times 400$ .

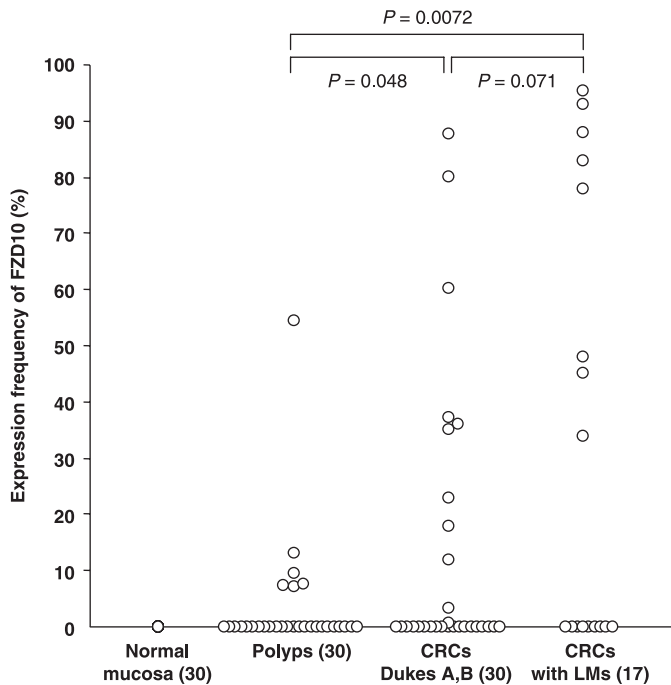


**Fig. 4.** Expression frequencies of Frizzled homolog 10 (FZD10) among three patient subgroups. (1) The 30 cases of colorectal polyps; (2) 30 colorectal cancer (CRC) cases of Dukes A and B that were followed-up and showed no evidence of recurrence for more than 5 postoperative years; and (3) the 17 CRC cases with synchronous liver metastases (LMs). There was a significant difference in FZD10 expression patterns among the three subgroups ( $P = 0.0008$ , ANOVA).

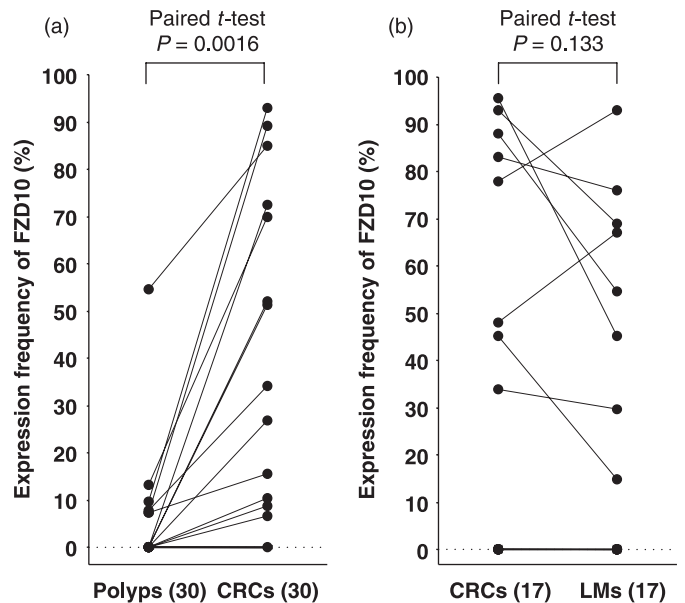


**Fig. 5.** Association of expression frequencies of Frizzled homolog 10 (FZD10) in paired samples. Expression frequencies of FZD10 were compared between colorectal polyps and coexisting colorectal cancers (CRCs) (a), and CRCs and synchronous liver metastases (LMs) (b) in the same patients (b).

one case of a polyp with an expression frequency as high as 54.5%, the frequency of the 30 CRC cases ( $20.5 \pm 31.7\%$ ) increased significantly as compared to coexisting polyps ( $3.3 \pm 10.3\%$ ) in paired samples from the same patient ( $P = 0.0016$ , paired *t*-test) (Fig. 5a). There was no correlation in expression frequencies between polyps and CRCs in paired samples from the same

patient (Pearson coefficient = 0.58). In contrast, there were no marked differences in expression frequencies between primary CRCs ( $33.2 \pm 39.7\%$ ) and metastatic liver lesions ( $26.4 \pm 33.4\%$ ) in paired samples from the same patient ( $n = 17$ ) ( $P = 0.133$ , paired  $t$ -tests) (Fig. 5b). A positive correlation in expression frequencies was evident between primary CRCs and metastatic liver lesions (Pearson coefficient = 0.90), indicating that FZD10-positive CRCs retained the property to produce FZD10-positive clones in metastatic lesions.

**Prognostic significance of FZD10 expression in CRCs.** The overall expression frequency of FZD10 in 104 curative resections for CRCs (mean age, 65.4 years) including Dukes A (30), B (26), C (31), and D with synchronous liver metastases (17) was  $14.1 \pm 26.8\%$ , and all patients could be divided into two groups (positive vs negative) with a cut-off frequency of 20%. There were no significant differences between the two groups for age, sex, tumor location (colon vs rectum), or Dukes classifications

(Student's  $t$ -tests and  $\chi^2$ -tests), although previous reports demonstrated that FZD10 expression was up-regulated by  $\beta$ -estradiol and retinoic acid.<sup>(15,16)</sup> With respect to overall survival rates, no significant differences were observed between the positive group with a greater than 20% frequency ( $n = 25$ ) and the other negative group ( $n = 79$ ) ( $P = 0.16$ , log-rank tests).

**Inverse association of FZD10 expression with nuclear  $\beta$ -catenin staining.** In the pathogenesis of CRCs, the activation of the canonical Wnt signaling pathway plays an important role, which is represented by the nuclear accumulation of  $\beta$ -catenin. In order to clarify whether FZD10-positive cancer cells showed the nuclear accumulation of  $\beta$ -catenin on a cellular level, we examined correlations in immunohistochemical expression patterns between FZD10 and  $\beta$ -catenin on the same cancer cell using serial sections of CRC specimens. Contrary to our expectation, almost all FZD10-positive cells were negative for nuclear  $\beta$ -catenin staining (Fig. 6a–d), whereas CRC cells with nuclear

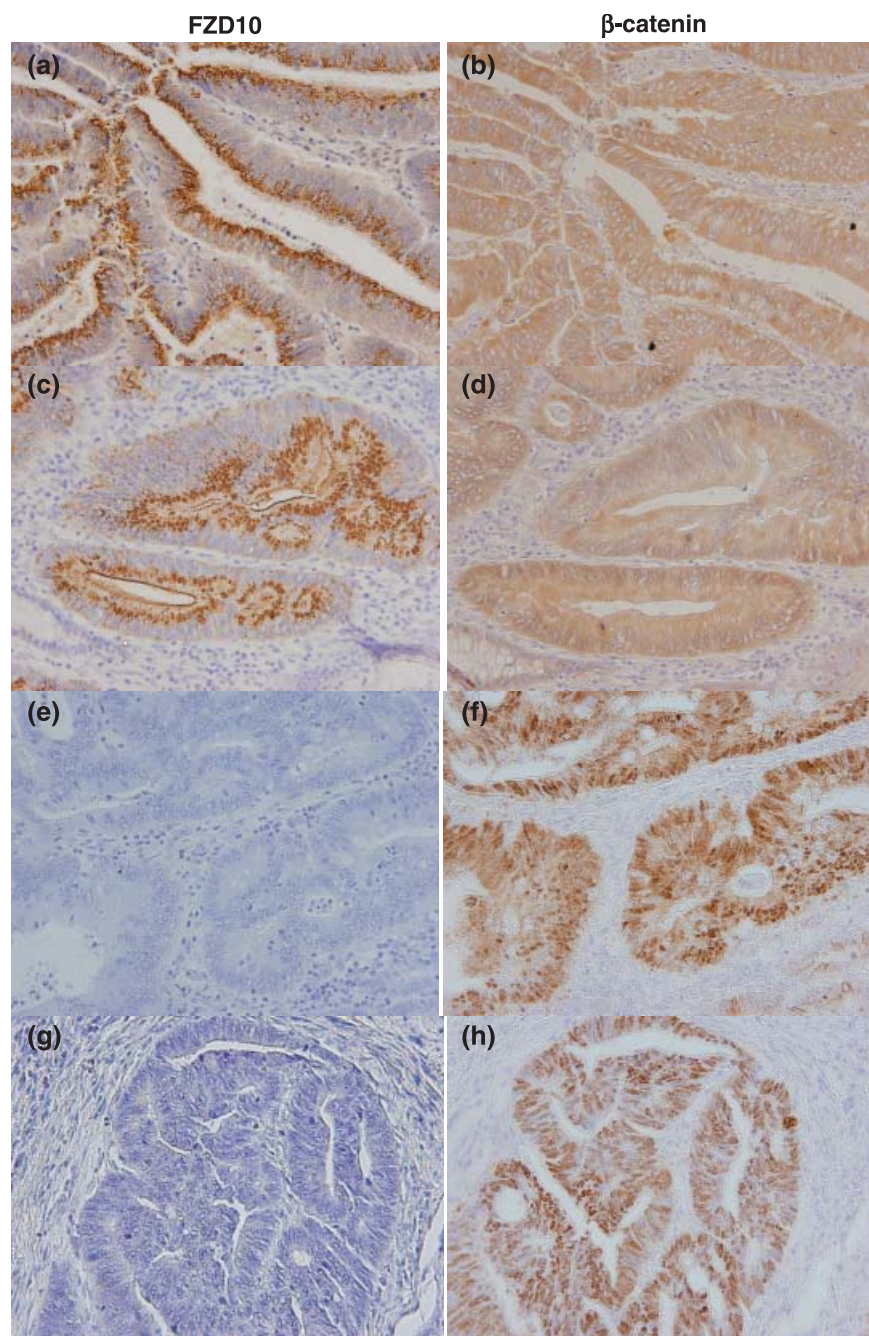


**Fig. 6.** The inverse correlation of Frizzled homolog 10 (FZD10) expression with the nuclear accumulation of  $\beta$ -catenin. Expression patterns of FZD10 (a, c, e, g) and  $\beta$ -catenin (b, d, f, h) were compared on serial sections, respectively, in FZD10-positive cases (a, c) and FZD10-negative cases (e, g). Original magnification:  $\times 400$ .

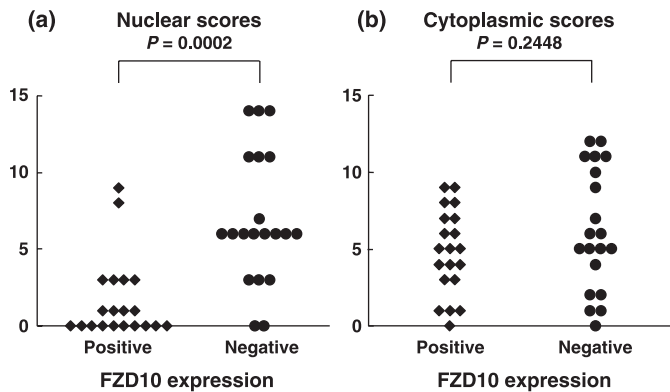


**Fig. 7.** Relationship between Frizzled homolog 10 (FZD10) expression and immunoreactive scores for  $\beta$ -catenin in colorectal cancers (CRCs). Twenty cases were randomly selected from each FZD10-positive and -negative CRC group. Each dot represents the immunoreactive score for  $\beta$ -catenin (nuclear or cytoplasmic) in cancer cells from one patient. There was a significant inverse correlation between expression patterns of FZD10 and  $\beta$ -catenin ( $P = 0.0002$ , Mann–Whitney tests); cancer cells immunopositive for FZD10 expression showed a significantly lower nuclear accumulation of  $\beta$ -catenin as compared to immunonegative cancer cells.

$\beta$ -catenin staining showed no FZD10 staining (Fig. 6e–h). When the staining intensity of  $\beta$ -catenin was semiquantified according to the subcellular localization, we found a strong inverse correlation between nuclear scores for  $\beta$ -catenin immunostaining and FZD10 expression patterns ( $P = 0.0002$ , Mann–Whitney tests) (Fig. 7a). There was no correlation between the cytoplasmic score for  $\beta$ -catenin immunostaining and the FZD10 expression status (Fig. 7b).

## Discussion

Little is known about the involvement of FZD10 in cancers, and we believe this study is the first to investigate the expression of FZD10 in a specific type of cancer using a large number of samples. The frequency of FZD10-positive tumors was almost equivalent in quantitative RT-PCR analyses (4/15 cases, 26.7%) and immunohistochemical analyses (25/104 cases, 24.4%), indicating that approximately one-quarter of CRCs may contain tumor cells with up-regulated FZD10 expression. The FZD10-positive rates were a little higher as compared to a previous report demonstrating that FZD10 expression was up-regulated in two out of 11 colorectal cancers by northern blotting.<sup>(12)</sup> We considered that the differences resulted from the sensitivity of the detection methods. Since the distribution of FZD10 expression has not been examined in colorectal cancers, our study provided a novel finding by immunohistochemical analysis that FZD10 was expressed exclusively in cancer cells and was absent in adjacent normal mucosal epithelium and stromal cells. Based on results from paired samples, the up-regulation of the *FZD10* gene may take place after polyps progress to CRCs. We found intratumoral as well as intertumoral heterogeneities for the FZD10 expression; even in CRCs evaluated as FZD10-positive cases not all tumor cells were positive for FZD10. This suggests a clonal evolution of FZD10-positive cells during the progression of primary CRCs. Intratumoral heterogeneities were also observed in liver metastatic lesions, and analyses of paired samples showed strong correlations between expression patterns of FZD10 in primary tumors and

metastatic liver lesions, indicating that primary CRCs with a given proportion of FZD10-immunopositive cells contained almost the same proportions of FZD10-immunopositive cells in corresponding metastatic lesions. These data suggest that a subset of CRCs may possess intrinsic genetic mechanisms causing the evolution of FZD10-positive clones, which have little advantage for developing metastasis.

Using *TRSEARCH* software based on the sequence database, the promoter region of the *FZD10* gene has several putative binding sites for different transcription factors including SP-1, GATA-2, and CdxA (data not shown). Although we could not find any particular clinical and pathological features distinguishing FZD10-positive tumors from FZD10-negative tumors, it may be related to a new subclassification of CRCs, and mechanisms which up-regulate the *FZD10* gene in a subset of tumor cells is an intriguing issue that needs to be further investigated.

To our surprise, we found a strong inverse correlation between FZD10 expression and nuclear  $\beta$ -catenin accumulation at the single-cell level, which contradicts the prevailing theory that in the pathogenesis of CRCs the Wnt signal via FZD receptors exerts its biological effect on tumor cells through the canonical pathway resulting in nuclear  $\beta$ -catenin accumulation. Although a previous experiment using *Xenopus* embryos showed that overexpression of FZD10 induced partial axis duplication possibly via  $\beta$ -catenin signaling pathway,<sup>(12)</sup> the correlation between FZD10 and  $\beta$ -catenin in human colorectal cancers has not been examined. Two hypotheses may be proposed to explain these results. The Wnt signal via the FZD10 receptor is transduced through the non-canonical pathway, such as the Wnt/Ca<sup>2+</sup> pathway, in which downstream molecules or events inhibit the nuclear accumulation of  $\beta$ -catenin. Examples of such negative cross-talk between canonical and non-canonical pathways have been demonstrated in the case of mouse *Fzd1*,<sup>(17)</sup> and human FZD6 receptors.<sup>(18)</sup> The other hypothesis is that when FZD10 is bound to its Wnt ligand it may disturb the endocytosis process of other FZD receptors which regulate the activity of downstream molecules such as the Dishevelled protein, thereby inhibiting the Wnt–FZD– $\beta$ -catenin pathway that is induced by other FZD receptors.<sup>(19)</sup> Forced expression of the FZD10 receptor in FZD10-negative CRC cells may provide clues to help answer this question. There was an intriguing report that K-ras activation increased the stability and nuclear accumulation of  $\beta$ -catenin,<sup>(20)</sup> and it is an interesting matter to investigate the relationship between FZD10 expression and K-ras activation, although no data on K-ras activation was available in the samples used in this study.

Although the function of FZD10 remains unclear, FZD10 may be a promising candidate molecule in the development of antibody-based diagnoses and treatments for liver metastases from CRCs. In metastatic liver lesions, FZD10 expression was not detected in liver parenchyma, and was confined to metastatic cancer cells. Combined with a novel imaging modality for high specificity, small foci containing FZD10-positive cells may be detected much earlier than by current modalities.<sup>(21)</sup> As for using FZD10 in treating CRC metastases, radioimmunotherapy using a specific monoclonal antibody directed against FZD10 is applicable, and promising effects have been demonstrated in a xenograft model of synovial sarcomas.<sup>(11)</sup> Since expression patterns in the primary and metastatic lesions were almost the same, it is possible to select a patient subgroup that may benefit from antibody treatment from expression findings of primary resected lesions.

## References

- 1 Sparks AB, Morin PJ, Vogelstein B, Kinzler KW. Mutational analysis of the APC/ $\beta$ -catenin/Tcf pathway in colorectal cancer. *Cancer Res* 1998; **58**: 1130–4.
- 2 Segditsas S, Tomlinson I. Colorectal cancer and genetic alterations in the Wnt pathway. *Oncogene* 2006; **25**: 7531–7.
- 3 Vincan E. Frizzled/WNT signalling: the insidious promoter of tumour growth and progression. *Front Biosci* 2004; **9**: 1023–34.

- 4 Reya T, Clevers H. Wnt signalling in stem cells and cancer. *Nature* 2005; **434**: 843–50.
- 5 Schneikert J, Behrens J. The canonical Wnt signalling pathway and its APC partner in colon cancer development. *Gut* 2007; **56**: 417–25.
- 6 Giles RH, van Es JH, Clevers H. Caught up in a Wnt storm: Wnt signaling in cancer. *Biochimica Biophysica Acta – Rev Cancer* 2003; **1653**: 1–24.
- 7 Holcombe RF, Marsh JL, Waterman ML *et al*. Expression of Wnt ligands and Frizzled receptors in colonic mucosa and in colon carcinoma. *Mol Pathol* 2002; **55**: 220–6.
- 8 Koji Ueno MH, Yutaka S, Shoichi H *et al*. Frizzled-7 as a potential therapeutic target in colorectal cancer. *Neoplasia* 2008; **10**: 697–705.
- 9 Nagayama S, Katagiri T, Tsunoda T *et al*. Genome-wide analysis of gene expression in synovial sarcomas using a cDNA microarray. *Cancer Res* 2002; **62**: 5859–66.
- 10 Nagayama S, Fukukawa C, Katagiri T *et al*. Therapeutic potential of antibodies against FZD10, a cell-surface protein, for synovial sarcomas. *Oncogene* 2005; **24**: 6201–12.
- 11 Fukukawa C, Hanaoka H, Nagayama S *et al*. Radioimmunotherapy of human synovial sarcoma using a monoclonal antibody against FZD10. *Cancer Sci* 2008; **99**: 432–40.
- 12 Terasaki H, Saitoh T, Shiokawa K, Katoh M. Frizzled-10, up-regulated in primary colorectal cancer, is a positive regulator of the WNT- $\beta$ -catenin – TCF signaling pathway. *Int J Mol Med* 2002; **9**: 107–12.
- 13 Krajewska M, Krajewski S, Epstein JI *et al*. Immunohistochemical analysis of bcl-2, bax, bcl-X, and mcl-1 expression in prostate cancers. *Am J Pathol* 1996; **148**: 1567–76.
- 14 Zimmermann KC, Sarbia M, Weber A-A, Borchard F, Gabbert HE, Schror K. Cyclooxygenase-2 expression in human esophageal carcinoma. *Cancer Res* 1999; **59**: 198–204.
- 15 Saitoh TMT, Katoh M. Up-regulation of Frizzled-10 (FZD10) by  $\beta$ -estradiol in MCF-7 cells and by retinoic acid in NT2 cells. *Int J Oncol* 2002; **20**: 117–20.
- 16 Katoh M. Regulation of WNT signaling molecules by retinoic acid during neuronal differentiation in NT2 cells: threshold model of WNT action. *Int J Mol Med* 2002; **10**: 683–7.
- 17 Roman-Roman S, Shi D-L, Stiot V *et al*. Murine Frizzled-1 behaves as an antagonist of the canonical Wnt/ $\beta$ -catenin signaling. *J Biol Chem* 2004; **279**: 5725–33.
- 18 Golan T, Yaniv A, Bafico A, Liu G, Gazit A. The human Frizzled 6 (HFz6) acts as a negative regulator of the canonical Wnt- $\beta$ -catenin signaling cascade. *J Biol Chem* 2004; **279**: 14879–88.
- 19 Bryja V, Cajanek L, Grahn A, Schulte G. Inhibition of endocytosis blocks Wnt signalling to  $\beta$ -catenin by promoting dishevelled degradation. *Acta Physiol* 2007; **190**: 55–61.
- 20 Li J, Mizukami Y, Zhang X, Jo W-S *et al*. Oncogenic K-ras stimulates Wnt signaling in colon cancer through inhibition of GSK-3 $\beta$ . *Gastroenterology* 2005; **128**: 1907–18.
- 21 Hama Y, Urano Y, Koyama Y *et al*. A Target cell-specific activatable fluorescence probe. for in vivo molecular imaging of cancer based on a self-quenched avidin-rhodamine conjugate. *Cancer Res* 2007; **67**: 2791–9.